



Original Article

# Establishment of a Rat Model of Liver Venous Deprivation: Simultaneous Portal and Hepatic Vein Ligation



Yuefeng Zhang<sup>1#</sup>, Xiaoqin He<sup>2#</sup>, Peng Ma<sup>1#</sup>, Liangkun Xiong<sup>1</sup>, Wenhui Bai<sup>1</sup>, Gaoshuo Zhang<sup>2</sup>, Yangtao Xu<sup>3</sup>, Wei Song<sup>3</sup> and Kaihuan Yu<sup>1\*</sup>

<sup>1</sup>Department of Hepatobiliary Surgery, Renmin Hospital of Wuhan University, Wuhan, Hubei, China; <sup>2</sup>Department of Teaching Office, Renmin Hospital of Wuhan University, Wuhan, Hubei, China; <sup>3</sup>The First Clinical College, Wuhan University, Wuhan, Hubei, China

Received: 18 January 2022 | Revised: 1 April 2022 | Accepted: 26 May 2022 | Published: 15 July 2022

## Abstract

**Background and Aims:** The aim was to establish a liver venous deprivation (LVD) model in rats, compare hepatic hypertrophy between LVD and associated liver partition and portal vein ligation for staged hepatectomy (ALPPS), and explore the underlying mechanisms. **Methods:** The LVD or extended-LVD (e-LVD) group received portal vein ligation (PVL) combined with hepatic vein ligation (HVL). The ALPPS or e-ALPPS group received PVL plus parenchyma ligation. Liver regeneration was assessed by measuring the liver weight and performing pathological analysis. Liver functions and the sphingosine kinase 1 (SPHK1)/sphingosine-1-phosphate (S1P)/sphingosine-1-phosphate receptor 1 (S1PR1) pathway were also investigated. **Results:** All future liver remnants (FLRs) in the ALPPS, e-ALPPS, LVD, and e-LVD groups exhibited significant hypertrophy compared with the control group. The LVD and e-LVD procedures induced similar liver hypertrophy than that in the corresponding ALPPS groups. Furthermore, the LVD and e-LVD methods led to obvious cytolysis in the venous-deprived lobes as well as a noticeable increase in serum transaminase levels, while no necrosis was observed in the ALPPS and e-ALPPS groups. SPHK1/S1P/S1PR1 pathway were distinctly activated after operation, especially in congestive/ischemic livers. **Conclusions:** We describe the first rat model of LVD and e-LVD with simultaneously associated HVL and PVL. Compared with the ALPPS

technique, the LVD or e-LVD procedure had a comparable overall effect on the hypertrophy response and a stronger effect on liver function. The SPHK1/S1P/S1PR1 pathway was involved in the LVD- or ALPPS-induced liver remodeling.

**Citation of this article:** Zhang Y, He X, Ma P, Xiong L, Bai W, Zhang G, et al. Establishment of a Rat Model of Liver Venous Deprivation: Simultaneous Portal and Hepatic Vein Ligation. J Clin Transl Hepatol 2023;11(2):393–404. doi: 10.14218/JCTH.2022.00032.

## Introduction

In cases of post hepatectomy liver failure caused by an insufficient future liver remnant (FLR), the “two- or multistage hepatectomy” strategy has been adopted. This approach modulates the liver to achieve an adequate FLR by the early-step procedure and performing major hepatectomy at a later stage.<sup>1–3</sup> Based on this concept, several liver preparation approaches have been proposed, such as portal vein ligation or embolization (PVL or PVE), associating liver partition and PVL for staged hepatectomy (ALPPS), and liver venous deprivation (LVD).<sup>1–4</sup> Those modulation methods were designed to enlarge the volume of the FLR and reduce the volume of the future liver excised (FLE). LVD was first introduced by Guiu et al.<sup>5</sup> in 2016, and the novel technique combined portal vein embolization (PVE) and hepatic vein embolization (HVE) via radiologic intervention during the same procedure. The same team also reported the extended-LVD (e-LVD) technique, which embolizes both the right hepatic vein (RHV) and middle hepatic vein (MHV) after PVE.<sup>6</sup> The LVD method simultaneously blocks PV inflow and HV outflow of the FLE and has an incremental effect on the FLR.<sup>5,6</sup> In some other studies, LVD was also reported as “radiological simultaneous porto-hepatic vein embolization” or “double embolization” for designating PVE and proximal embolization of one hepatic vein.<sup>7,8</sup>

PVE has become a widely used but inefficient approach to stimulate hypertrophy of FLR, and the ALPPS procedure seems to be more aggressive and efficient but is accompanied by more complications.<sup>1–3,9</sup> The safety and efficacy of LVD remain unclear because of a relatively limited number of studies. A recent multicenter study compared LVD with PVE and reported that LVD achieved better FLR

**Keywords:** Hepatectomy; Portal vein; Hepatic vein; Hypertrophy; Animal model.

**Abbreviations:** α-SMA, α-smooth muscle actin; ALB, albumin; ALT, alanine aminotransferase; ALPPS, associating liver partition and portal vein ligation for staged hepatectomy; AST, aspartate aminotransferase; BC, blank control; CL, caudate lobe; ELISA, enzyme-linked immunosorbent assay; e-LVD, extended liver venous deprivation; FLE, future liver excised; FLR, future liver remnant; GS, glucose and sodium chloride; H-E, hematoxylin-eosin; HV, hepatic vein; HVE, hepatic vein embolization; HVL, hepatic vein ligation; LLL, left lateral lobe; LMHV, left median hepatic vein; LML, left median lobe; LMPV, right median portal vein; LVD, liver venous deprivation; MMHV, middle median hepatic vein; POD, postoperative day; PP, pericaaval parenchyma; PV, portal vein; PVE, portal vein embolization; PVL, portal vein ligation; RIL, right inferior lobe; RMHV, right median hepatic vein; RML, right medial lobe; RMPV, right median portal vein; RSL, right superior lobe; Tp-ALPPS, tourniquet partial-ALPPS; S1P, sphingosine-1-phosphate; S1PR1, sphingosine-1-phosphate receptor 1; SPHK1, sphingosine kinase 1.

\*Contributed equally to this work.

\*Correspondence to: Kaihuan Yu, Department of Hepatobiliary Surgery, Renmin Hospital of Wuhan University, Wuhan, Hubei 430060, China. ORCID: <https://orcid.org/0000-0001-9235-7848>. Tel: +86-13517282628, E-mail: 13517282628@163.com

**Table 1. Hepatic vein ligation and hepatic vein embolization interventions in different species**

Species	Author and year	Designation	Gross appearances	Microscopic findings of FLE
Human	Guiu <i>et al</i> , 2016 <sup>5</sup>	Combined right portal vein and right hepatic vein embolization	The right lobe was discolored (darker) and atrophied, the left liver lobe was enlarged, and there was definite line between the two	Atrophy of hepatocytes and dilatation of centro- and medio-lobular and sinusoids hepatocyte zonal necrosis
Rabbit	van Lienden <i>et al</i> , 2011 <sup>12</sup>	Embolization both the HV and PV of the cranial liver lobes	Unclear	Periportal sinusoidal dilation in conjunction with atrophy of the hepatocytes and local necrosis
Pig	Schadde <i>et al</i> , 2019 <sup>13</sup>	Combination PV (for RML, LML and LLL) and HV (for RML, LML and LLL) ligation	The volume of portal vein-supplied sector increased, and the deportalized sectors were atrophied	No evidence of hepatocyte necrosis
Rat	Kawaguchi <i>et al</i> , 2019 <sup>14</sup>	Combination PV (for RML, LML and LLL) and HV (for LLL) ligation	Unclear	In POD 1, hepatocyte atrophy, sinusoidal congestion, and cytoplasmic vacuolation were observed. In POD 7, fibrosis ensuing was found.

FLE, future liver excised; HV, hepatic vein; HVE, hepatic vein embolization; LLL, left lateral lobe; LML, left median lobe; POD, postoperative day; PV, portal vein; PVE, portal vein embolization; RML, right medial lobe.

hypertrophy (59% vs. 48%;  $p=0.020$ ) and resectability (90% vs. 68%;  $p=0.007$ ) than PVE.<sup>10</sup> Another retrospective study compared the hypertrophy efficacy, feasibility and safety between LVD and ALPPS and showed that the increase in the FLR volume was similar after LVD and ALPPS (63% vs. 56%;  $p=0.727$ ), and the successful resection rate was significantly lower after LVD than after ALPPS (72.6% vs. 90.6%,  $p<0.001$ ).<sup>11</sup> However, more prospective clinical studies with larger samples are needed to comprehensively compare these different liver modulation procedures.

Animal models are useful for observing the pathophysiological effects and investigating the underlying mechanisms of LVD. As shown in Table 1, van Lienden *et al.*<sup>12</sup> described a rabbit model of PVE and HVE in 2012, but no short-term additive effect on FLR hypertrophy was observed. Schadde *et al.*<sup>13</sup> in 2019 developed a porcine model of LVD by surgical ligation of the HV and PV, and found that compared with PVL alone, LVD accelerated hepatic hypertrophy. In 2019, Kawaguchi *et al.*<sup>14</sup> described a rat model that combined PVL and hepatic venous congestion in the liver, and the caudate lobe (CL) was designed as FLR. However, the CL is naturally isolated and has no collaterals with other lobes, so that mode is not suitable for use as an LVD model. Because rodents are readily available to general researchers, we attempted to establish LVD and e-LVD models in rats and compared hepatic hypertrophy induced by LVD and ALPPS.

## Methods

### Animals

Inbred male Sprague–Dawley rats were obtained from Hunan SJA laboratory animal Co., Ltd (Changsha, China) and, 8 to 10 weeks of age and were housed under specific pathogen-free conditions. Studies have confirmed that liver regeneration is partially regulated by sex; thus, males were used to exclude the influence of sex hormone cycles.<sup>15</sup> The rats were provided *ad libitum* access to standard rat chow and water. All animal procedures and housing were conducted following current regulations and guidelines. This animal procedures were approved by the Ethics Committee of the Animal Experiment Center of Wuhan University.

### Experimental design

The rats were randomly allocated to six groups, a blank control (BC) group, control group, LVD group, e-LVD group, ALPPS group, and e-ALPPS group. The BC group included six healthy untreated rats. Baseline of body weight, liver weight, and liver enzyme levels were determined. The interventions received by the control rats and the other experimental groups are listed in Table 2. The ALPPS and e-ALPPS models corresponded to the LVD and e-LVD models, respectively. The animals were sacrificed on postoperative days (POD) 2, 4, and 7 ( $n=3$  rats per group on POD 2 and 4;  $n=5$  rats per group on POD 7).

### Surgical procedures

Anesthesia was administered by inhalation of a mixture of oxygen and isoflurane (RWD Life Science, Shenzhen, China). After shaving the hair and disinfecting the skin, a 6.0 cm midline incision was performed to expose the liver lobes, hepatic pedicle, and hepatic veins. After the operation, each animal received an injection of 6 mL of a 5% glucose and sodium chloride (GS) solution containing 0.96 mg gentamicin. The interventions in the six groups are listed in Table 2. The PV supplying the right lobe (RL) was ligated in the ALPPS, LVD, e-ALPPS and e-LVD groups, and the RL remained. These rats were weighed immediately after surgery (POD 0).

**PVL:** PVs were dissected with fine forceps and ligated or sutured with 5-0 nylon thread. The accompanying artery and bile duct were carefully protected.

**Resection of liver lobes:** Because the portal vein branch of the CL was difficult to separate, we chose to remove the CL. The left lateral lobe (LLL, approximately 44% of the total liver, Fig. 1B) was so large that a large amount of blood accumulated in the LLL after left HVL, which eventually leads to shock, thus the LLL was also excised. The CL and LLL were removed with scissors after ligating their roots.

**HVL:** In rats, the middle median hepatic vein (MMHV) merges with the left median hepatic vein (LMHV) to form the common trunk (Fig. 2A). An obvious pouch was identified between the right median hepatic vein (RMHV) and the common trunk at the second hepatic hilum, and the pit

**Table 2. Interventions in the study groups**

Group	Number of animals	Numbers of survivors	Removal of the CL and LLL	Ligation of the RMPV	Ligation of the LMPV	Parenchymal ligation	Ligation of the RMHV	Ligation of the common trunk	FLR	FLE
BC	6	–	–	–	–	–	–	–	–	–
Control	11	11	+	–	–	–	–	–	–	–
ALPPS	11	11	+	+	–	+	–	–	LML	RML
LVD	11	11	+	+	–	–	+	–	LML	RML
e-ALPPS	11	11	+	–	+	+	–	–	RML	LML
e-LVD	14	11	+	–	+	–	–	+	RML	LML

"+" indicates "yes"; "–" indicates no. ALPPS, associating liver partition and portal vein ligation for staged hepatectomy; BC, blank control; CL, caudate lobe; e-LVD, extended liver venous deprivation; FLE, future liver excised; FLR, future liver remnant; LLL, left lateral lobe; LML, left median lobe; LMPV, right median portal vein; LVD, liver venous deprivation; RMHV, right median hepatic vein; RML, right medial lobe; RMPV, right median portal vein.

was an important and useful anatomical marker (Fig. 3A). Specifically, the hepatic capsule at the pit was penetrated with curved tweezers, and the tips of the tweezers passed through the liver parenchyma between the inferior vena cava and the LMHV or RMHV. The silk suture was inserted with tweezers, and then the HV was ligated (Fig. 2C).

**Parenchymal ligation between the LML and RML:** Tourniquet partial ALPPS (Tp-ALPPS) is recognized as a novel variant of the classic ALPPS procedure that replaces parenchymal transection by placing a liver tourniquet across the liver parenchyma through an avascular region.<sup>16</sup> We applied the Tp-ALPPS procedure using the parenchymal ligation method when developing the ALPPS model in this study. Specifically, after PVL, the demarcation line usually occurred slightly to the left of the falciform ligament, and then the entire parenchyma of the LML was penetrated with curved tweezers from the diaphragmatic side to the visceral side along the plane of the demarcation line. To protect the MMHV, the insertion point was selected approximately 5 mm anterior to the inferior vena cava. The exit point was located at the junction of the left and right bile ducts (Fig. 2B). Then, a 4-0 silk suture was inserted with tweezers, and the parenchyma was ligated with a proper amount of strength.

### Liver evaluation, weighing, and sampling

On POD 2, 4, and 7, the rats were euthanized painlessly with bleeding under anesthesia. Blood from the rats was collected into serum tubes (BD Biosciences, NJ, USA) via puncture of the abdominal aorta, and serum was obtained with a standard procedure and stored at –20°C until use. All perihepatic vessels and ligaments were cut to harvest the whole liver. The weight of each individual liver lobe was measured and recorded. Part of this liver tissue was stored at –80°C until use. The liver growth ratio was calculated using as follows:

Growth ratio =

$$\frac{\text{Actual liver lobe weight} - \text{Initial body weight} * \frac{\text{Liver lobe weight of BC group}}{\text{Body weight of BC group}}}{\text{Initial body weight} * \frac{\text{Liver lobe weight of BC group}}{\text{Body weight of BC group}}}$$

### Plasma values

The serum liver enzyme levels, including aspartate aminotransferase (AST), alanine aminotransferase (ALT), and albumin (ALB), were assayed with a serum multiple biochemical analyzer (Siemens, Berlin, Germany).

### Pathological analysis

The LML and RML liver tissues were fixed with 4% formalin and embedded in paraffin. A tissue microarray was constructed from the specimens, which were sectioned and mounted onto slides. Routine hematoxylin-eosin (H-E) staining was performed to observe structural changes. Immunostaining was also performed in the tissue sections, Ki-67 (Proteintech, Wuhan, China) was used as a marker of hepatocyte regeneration,  $\alpha$ -smooth muscle actin ( $\alpha$ -SMA, Proteintech, Wuhan, China) was used to identify myofibroblasts.<sup>17,18</sup> Extracellular collagen fibers were stained with picric acid-sirius red.<sup>19</sup> All sections were digitally imaged using a slide scanner (Hamamatsu Electronic, Shizuoka-ken, Japan). Quantitative evaluation of Ki-67 staining was performed. Briefly, the number of Ki-67-positive hepatocytes per 1,000 hepatocytes were counted in six randomly selected visual fields (200 $\times$ ).

### Measurement of sphingosine-1-phosphate (S1P)

Liver tissue was homogenized with an ultrasonic crusher and the supernatant was separated by centrifugation. S1P in supernatants and serum was measured using an enzyme-linked immunosorbent assay (ELISA) kit (Cloud-clone, Wuhan, China) following standard procedures.

### Western blot assays

Protein levels were determined by standard western blot assays. Liver tissue proteins were extracted with RIPA buffer containing protease inhibitors (Beyotime, Beijing, China) and quantified with Pierce BCA Protein Assay Kit (Thermo Fisher, MA, USA). These protein samples were resolved by 10% sodium dodecyl sulfate-polyacrylamide gel electrophoresis and transferred to polyvinylidene difluoride membranes (Bio-Rad, CA, USA). Rabbit anti-sphingosine kinase 1 (SPHK1), anti-sphingosine-1-phosphate receptor 1 (S1PR1), and GAPDH (Proteintech, Wuhan, China) were used. Densitometry analyses of western blot were conducted with Image-J software (NIH, MD, USA).

### Statistical analysis

Quantitative data were reported as means with standard deviation and were analyzed using GraphPad Prism 6.0 software (La Jolla, CA, USA). Differences between groups were compared with two-way analysis of variance. Stu-

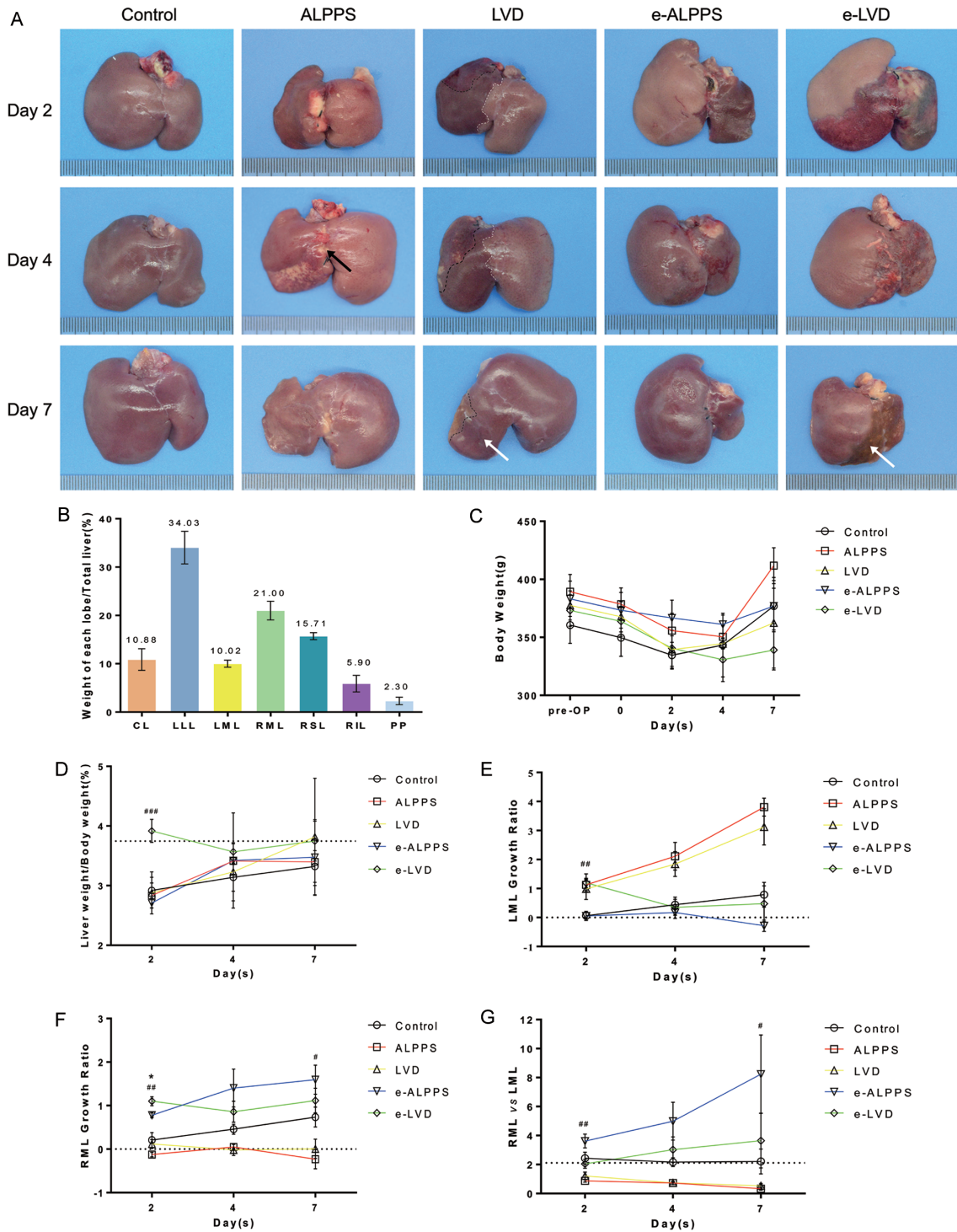


**Fig. 1. Liver remodeling after different surgeries.** (A) Changes in the appearance of the liver middle lobes after surgery on POD 2, 4, and 7. The white dotted line is the dividing line between the supply territories of the RMPV and LMPV, and the black dotted line is the dividing line between the drainage areas of the RMHV and MMHV. Area H is the sector surrounded by the dotted lines. The black arrow indicates the necrosis zone after parenchymal ligation. The white arrow indicates area H. (B) Analysis of the relative weights of each rat liver lobe compared to the total liver weights in the BC rats. (C) Changes in body weight at each time point. (D) Weight of the remnant liver/body weight evolution; the dotted line ( $Y=3.75$ ) denotes the total liver weight/body weight in the BC rats. (E) and (F) The weight changes in RML and LML were reported with growth ratios. (G) The RML/LML ratio reflects the morphological changes in the middle lobes after surgery. The dotted line ( $Y=2.11$ ) denotes the RML/LML in the BC rats. (\*ALPPS vs. LVD; #e-ALPPS vs. e-LVD. \*or  $p < 0.05$ ; \*\*or  $p < 0.01$ ; \*\*\*or  $p < 0.001$ ). ALPPS, associating liver partition and portal vein ligation for staged hepatectomy; BC, blank control; CL, caudate lobe; e-LVD, extended liver venous deprivation; FLE, future liver excised; FLR, future liver remnant; LLL, left lateral lobe; LML, left median lobe; LMPV, right median portal vein; LVD, liver venous deprivation; MMHV, middle median hepatic vein; RML, right medial lobe; RSL, right superior lobe; RMHV, right median hepatic vein; RMPV, right median portal vein.

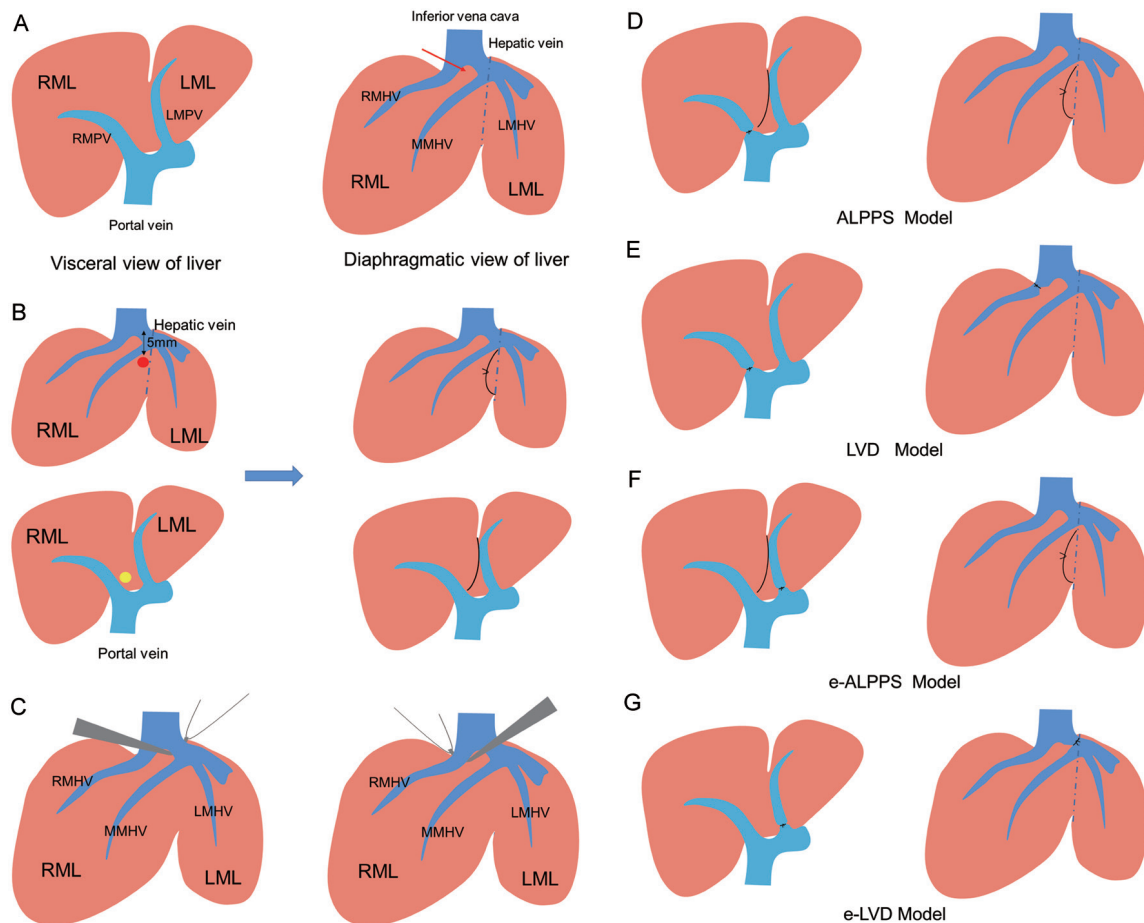


**Fig. 2. Schematic of different rat models.** The portal (left panel) and hepatic (right panel) vein anatomy of the RML and LML are shown. The blue dotted line indicates the falciform ligament of the liver. (A) Parenchymal ligation between the LML and RML is shown with a red dot indicating the entry point and a yellow dot indicating the exit point of the silk suture. (B) Ligation of the RMHV (left panel) and common trunk of the MMHV and LMHV (right panel) were performed with curved tweezers to carry the silk suture. (D–E) Diagrams of the ALPPS, LVD, e-ALPPS, and e-LVD models. ALPPS, associating liver partition and portal vein ligation for staged hepatectomy; e-LVD, extended liver venous deprivation; LMHV, left median hepatic vein; LML, left median lobe; LMPV, right median portal vein; LVD, liver venous deprivation; MMHV, middle median hepatic vein; RMHV, right median hepatic vein; RML, right medial lobe; RMPV, right median portal vein.

dent's *t*-test was used to analyze the differences between two groups. *P*-values <0.05 was considered statistically significant.

## Results

### New models of LVD, e-LVD, ALPPS, and e-ALPPS in rats

We took advantage of the liver venous system of the LML and RML in rats, which is similar to that in humans, and designed LVD and e-LVD rat models as well as ALPPS and e-ALPPS models (Fig. 2D–G). As shown in Fig. 3D, after PVL, a clear demarcation line emerged between the LML and RML in all the experimental groups, and the FLE lobe turned dark red due to ischemia. Next, upon ligation of the hepatic vein, the FLE lobes turned from dark red to black red and became swollen due to congestion. The congested area was significantly smaller than the ischemic area in the LVD group, but was significantly larger than that in the e-LVD group. After the operation, all rats presented as energetically dispirited and had slow reactions, reduced feeding, and little move-

ment in the first few days. Pale skin (ears and toes) was only observed in the e-LVD group. No perioperative mortality was observed in the control, ALPPS, LVD, and e-ALPPS groups, while the survival rate after surgery in the e-LVD group was 78.57% (14 animal surgeries were completed, and 11 animals survived), which was significantly lower than that in the other groups.

### Postoperative follow-up, remodeling of the liver shape

Due to surgical stress, the body weight loss reached a maximum of approximately  $7.2 \pm 3.1\%$  on POD 2 and began to recover in the control group. In the experimental groups, body weight reached the lowest point on POD 4. The e-LVD group had a loss of  $11.62 \pm 5.0\%$  of body weight on POD 4 and only recovered to  $90.9 \pm 4.6\%$  on POD 7 (Fig. 1C).

Gross views of the RML and LML in the different groups are shown in Figure 1A. In the control group, both the RML and LML edges became blunt, and they had a relatively constant proliferation speed and a similar degree of hyperplasia (Fig. 1A, G). In contrast, The ALPPS and LVD groups had significantly greater hypertrophic effects on the FLR lobe (LML)

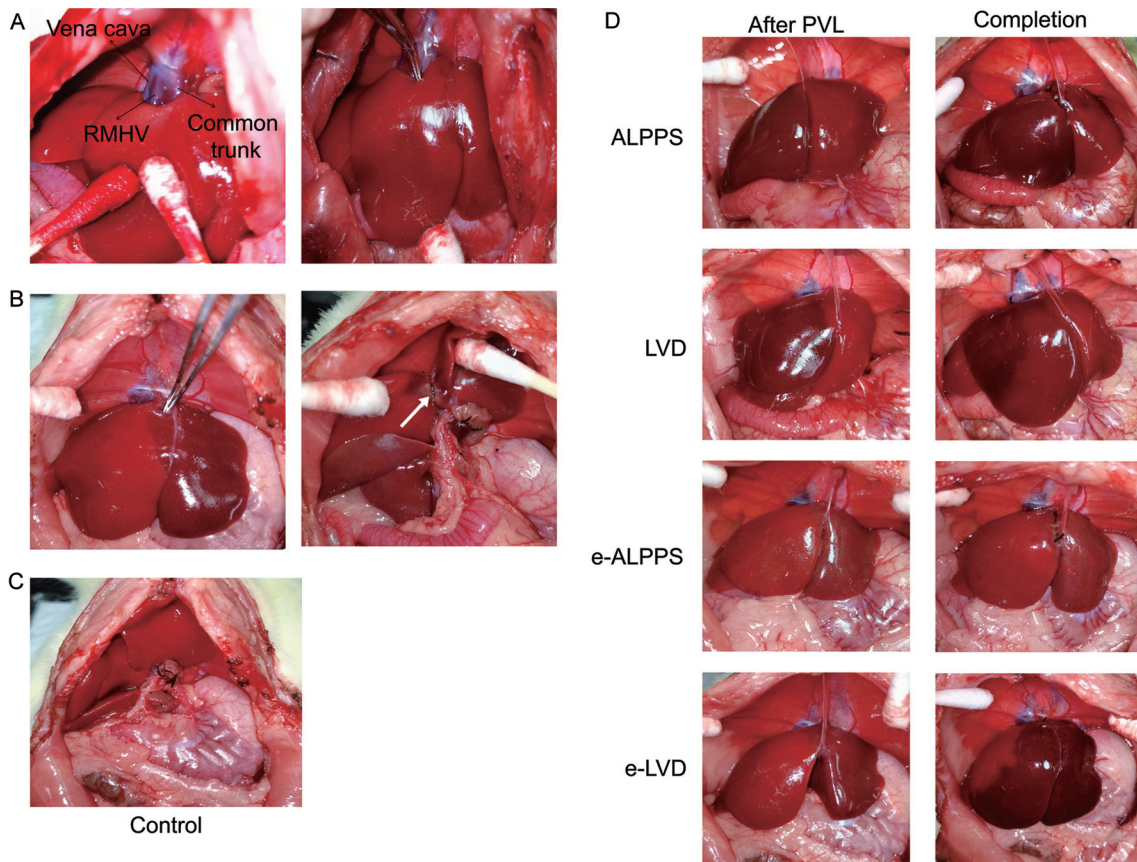


**Fig. 3. Surgical procedures used in different rat models.** (A) The second hepatic hilum of the rat liver. The tweezer tip indicates the natural pit located between the RMHV and common trunk, which is an important anatomical landmark. (B) Parenchymal ligation between the LML and RML. The ligation plane on the ML was slightly to the left of the demarcation line. The tweezer tip indicates the entry point, and the white arrow indicates the ligature. (C) representative pictures of the control group. The LLL and CL were removed in all the groups. (D) Pictures of the ALPPS, LVD, e-ALPPS, and e-LVD models. The left panel shows the demarcation that emerged after PVL. The left panel shows changes in the liver after HVL or parenchymal ligation. Congestion occurred in the LVD and e-LVD groups. ALPPS, associating liver partition and portal vein ligation for staged hepatectomy; CL, caudate lobe; e-LVD, extended liver venous deprivation; HVL, hepatic vein ligation; LLL, left lateral lobe; LML, left median lobe; LVD, liver venous deprivation; RML, right medial lobe; RMHV, right median hepatic vein.

than in the control group on POD 7 (growth ratio:  $3.80 \pm 0.31$ ,  $3.12 \pm 0.62$  vs.  $0.79 \pm 0.43$ ,  $p < 0.001$ ). No significant difference was observed between the ALPPS and LVD groups ( $p = 0.0591$ , Fig. 1E). Moreover, the FLE lobe (RML) in the ALPPS and LVD groups had different degrees of hypotrophy (growth ratio:  $-0.23 \pm 0.22$  and  $0.01 \pm 0.22$ ), and the venous-deprived sector in the LVD group exhibited obvious atrophy (Fig. 1F). Consequently, the RML/LML was reversed, and the liver shape was dramatically changed (Fig. 1A, G).

Similarly, accelerated regeneration of the FLR lobe (RML) was observed in the e-ALPPS and e-LVD groups compared with the control group (growth ratio:  $1.60 \pm 0.33$ ,  $1.11 \pm 0.28$  vs.  $0.79 \pm 0.43$ ,  $p < 0.001$ ), and a significant difference was observed between the e-ALPPS and e-LVD groups ( $p = 0.0397$ , Fig. 1F). Moreover, the size of the FLE lobe (LML) was decreased (growth ratio:  $-0.28 \pm 0.19$ ) in the e-ALPPS group but was slightly increased in the e-LVD group (growth ratio:  $0.47 \pm 0.67$ ), which may have resulted from hepatic venous congestion (Fig. 1A, E).

### Changes in microstructure after surgery

Tissue structure was evaluated in sections of both the FLE and FLR lobes in each group (Fig. 4A). As shown in Figure 4B, D, and Supplementary Figure 1, hepatocytes the FLR lobes in

both groups were enlarged and crowded, and more hepatocytes were positive for nuclear Ki-67, a marker of mitosis, in both groups. In addition, the peak of Ki-67 expression occurred on POD 2. Notably, Ki-67 was expressed at approximately 3-fold higher levels in the experimental groups than in the control group, and no significant differences were observed among the experimental groups (Fig. 4D). There was evidence that more hepatocytes entered the cell cycle in the experimental groups than in the control group.

Regarding the FLE in the LVD and e-LVD groups, a large confluent area of necrosis, obscured lobular structure, and scattered viable hepatocyte islands were observed 2 days after venous deprivation. The necrotic area was gradually replaced with fibrous tissue, and the process of scar healing was nearly completed on POD 7 (Fig. 4B and Supplementary Fig. 2). The fibrous tissues were further confirmed by the  $\alpha$ -SMA and picric acid-sirius red staining (Fig. 4C). In contrast, no evidence of necrosis or cytoplasmic degeneration was found in the ALPPS and e-ALPPS groups (Fig. 4B).

### Liver enzymes

Serum ALT and AST levels and hepatocyte injury markers were measured. As shown in Figure 5A, B, the ALPPS and e-ALPPS procedures affected liver function and were accom-

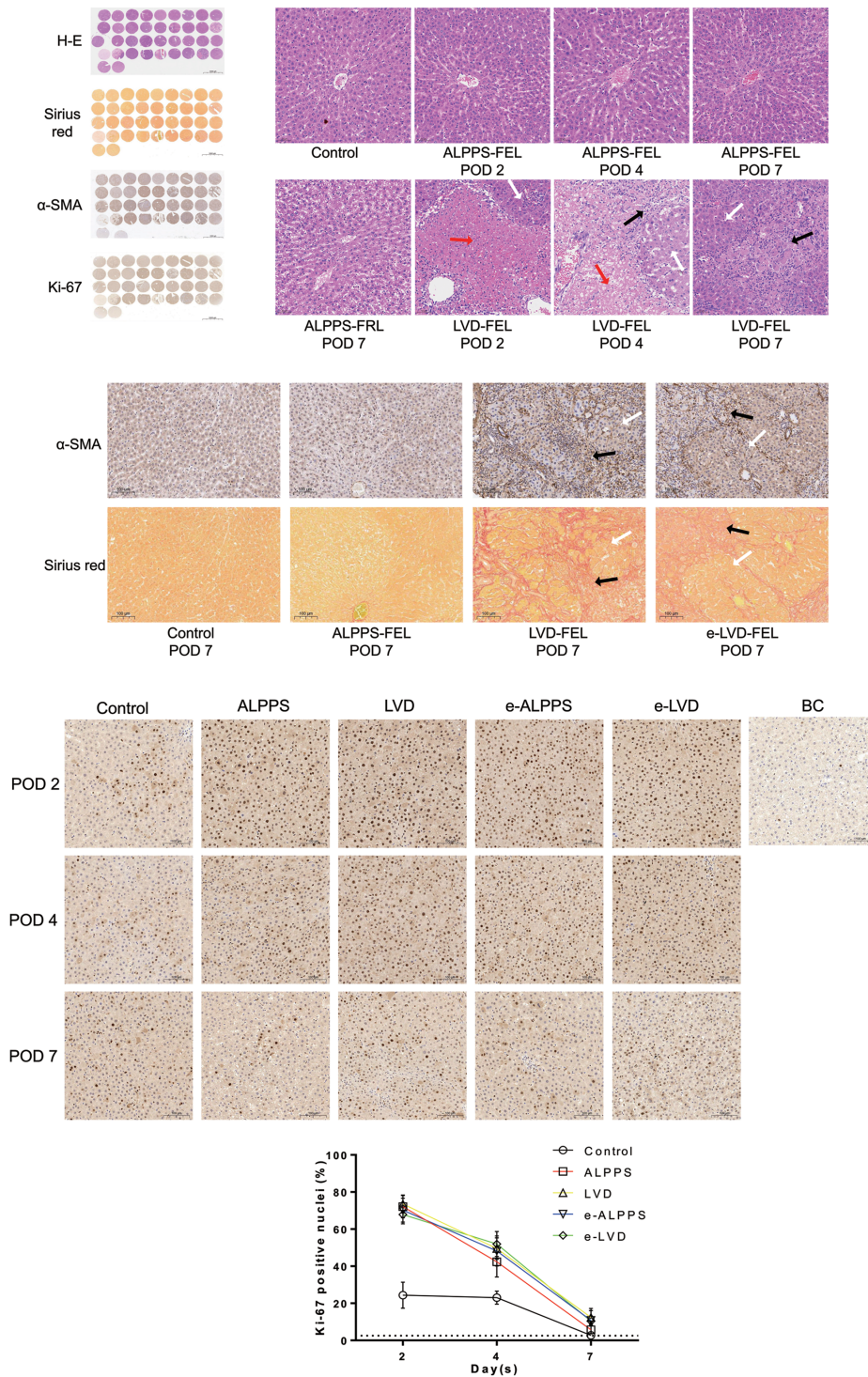


**Fig. 4. Histological examination of the liver after surgery.** (A) Tissue from harvested livers was stained with hematoxylin and eosin (upper), picric acid–sirius red and α-SMA (middle) and Ki-67 (lower). (B) FLRs of the ALPPS, LVD, e-ALPPS, and e-LVD groups had similar changes. A representative image of hematoxylin and eosin staining in the FLR from the ALPPS group on POD 7 is shown. The FLE of the ALPPS and e-ALPPS groups had a different appearance from that in the e-LVD and LVD groups, but the FLE in the e-LVD and LVD groups had similar changes. Representative images of hematoxylin and eosin-stained FLE in the ALPPS and LVD group on days 2, 4 and 7 are shown. White, red, and black arrows indicate viable hepatocyte islands, necrotic areas, and fibrous tissues, respectively. (C) α-SMA and picric acid–sirius red were used to stain the myofibroblasts and extracellular collagen fibers. Hepatocyte islands (white arrows) indicate the and fibrous tissue (black arrows) are shown. (D) Representative images (200×) of Ki-67 immunohistochemical staining in each group. The numbers of Ki-67-positive cells in the FLR after surgery are shown. The dotted line (Y=2.5) denotes the percentage of Ki-67-positive cells. (\*ALPPS vs. LVD; #e-ALPPS vs. e-LVD. \*or #p<0.05; \*\* or ##p<0.01; \*\*\* or ###p<0.001). α-SMA, α-smooth muscle actin; ALPPS, associating liver partition and portal vein ligation for staged hepatectomy; BC, blank control; e-LVD, extended liver venous deprivation; FLE, future liver excised; FLR, future liver remnant; H-E, hematoxylin-eosin; LVD, liver venous deprivation; POD, postoperative day.

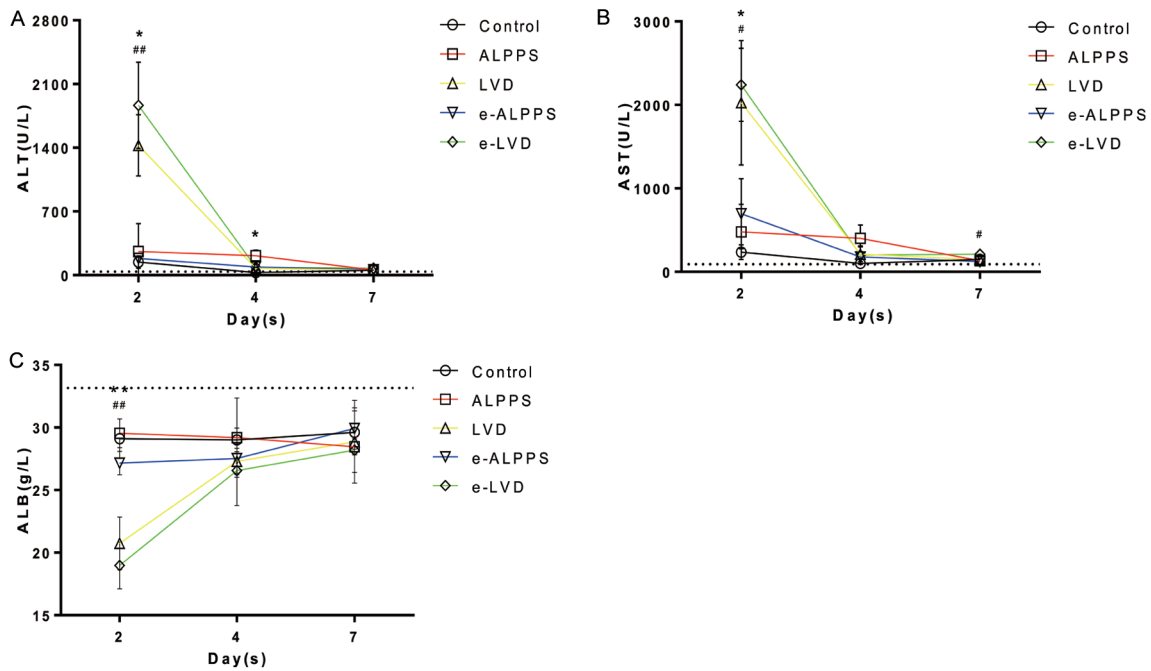


**Fig. 5. Changes in liver enzyme levels before and after surgery.** (A–C) Liver function and injury evaluated by serum AST (A), ALT (B) and ALB (C). Dotted lines ( $Y=39.33$ ,  $91.67$  and  $33.17$ ) show serum AST, ALT, and ALB levels, respectively, in the BC rats. (\*ALPPS vs. LVD; #e-ALPPS vs. e-LVD. \* or # $p<0.05$ ; \*\* or ## $p<0.01$ ; \*\*\* or ### $p<0.001$ ). ALB, albumin; ALT, alanine aminotransferase; ALPPS, associating liver partition and portal vein ligation for staged hepatectomy; AST, aspartate aminotransferase; BC, blank control; e-LVD, extended liver venous deprivation; LVD, liver venous deprivation; POD, postoperative day.

panied by increased ALT and AST levels. Both the ALT and AST levels in the LVD and e-LVD groups were significantly higher on POD 2 than those in the ALPPS ( $1,427.67\pm336.53$  vs.  $259.33\pm131.18$ ,  $p<0.001$ ;  $2,025.67\pm746.42$  vs.  $479.67\pm329.99$ ,  $p<0.001$ ) and e-ALPPS ( $1,864.33\pm475.75$  vs.  $184.33\pm37.64$ ,  $p<0.001$ ;  $2,242.33\pm437.50$  vs.  $696.00\pm419.42$ ,  $p<0.001$ ) groups, respectively. All levels returned to baseline on day 7 (Fig. 5A, B). The metrics of liver synthetic function were evaluated by measuring ALB levels. ALB showed the opposite trend, and declined substantially to  $20.73\pm2.10$  g/L and  $18.97\pm1.88$  g/L in the LVD and e-LVD groups, respectively (Fig. 5C). However, ALB levels were slightly decreased in the other groups. Notably, the ALB levels did not return to normal even on POD 7 (Fig. 5C).

#### Activation of the SPHK1/S1P/S1PR1 pathway

To confirm the involvement of the SPHK1/S1P/S1PR1 pathway in LVD- or ALPPS-induced liver regeneration, the levels of SPHK1/S1P/S1PR1 were examined. As shown in Figure 6A, S1P serum and liver concentrations were significantly elevated in the experimental groups on POD 2 ( $p<0.05$ ), and the S1P levels in FLE were significantly higher than that in FLR ( $p<0.05$ ), which implied that congestive or ischemic liver (FLE) produced more S1P than the FLR. The western blot results showed that the expression of SPHK1 and S1PR1 was significantly upregulated in the FLE compared with the FLR.

#### Discussion

LVD promotes curative hepatectomy previously limited by an insufficient FLR volume.<sup>5,6</sup> Guiu *et al.*<sup>5,6</sup> first reported a series of LVD and e-LVD cases in 2016 and 2017. Schadde

*et al.*<sup>13</sup> established a true LVD model in swine in 2018. In this study, we established a feasible, reproducible LVD model in rats. The distinction between the LVD and e-LVD should be discussed first. During the LVD technique in the clinic, the RHV and RPV are usually simultaneously embolized, but in e-LVD, the MHV is embolized in addition to the RHV and RPV.<sup>5,6</sup> The drainage area of the HV does not match the supply area of the PV. For example, segment 4 in the human liver is supplied by the LPV and drained by the MHV. Therefore, for LVD, the drainage area of the blocked HV is less than the supply area of the embolized PV, and for e-LVD, the drainage area of the occluded HV is larger than the supply area of the embolized PV.<sup>5,6</sup>

Most of the rat liver lobes, except for the LML and RML, are naturally separated and have a relatively independent Glisson system and HV system. The LML and RML were selected as the observational objects because their anatomical structure is similar to that the human liver. As shown in Figure 2A, the LML and RML were supplied by the LMPV and RMPV, respectively. The LML was drained by the LMHV, and the RML was drained by the RMHV and MMHV. The MMHV merged with the LMHV to form a common trunk. A small depression was observed between the common trunk and the RMHV in front of the inferior vena cava (Figs. 2A and 3A). When establishing the LVD model, the RMHV and RMPV were ligated simultaneously (Fig. 2E). The most appropriate models for e-LVD should combine RMPV ligation with ligation of both the RMHV and MMHV, but the MMHV is deeply embedded in the parenchyma and close to some large veins (Fig. 2A). Dissection of the MMHV usually causes uncontrollable bleeding. As a result, for the e-LVD model, the common trunk and LMPV were ligated simultaneously (Fig. 2G) and the drainage area of the occluded HV was larger than the supply area of the ligated PV. In response to the LVD and e-LVD models, the ALPPS and e-ALPPS models were built by ligating the RMPV and LMPV, respectively. In addition, the collateral branches between the LML and RML were

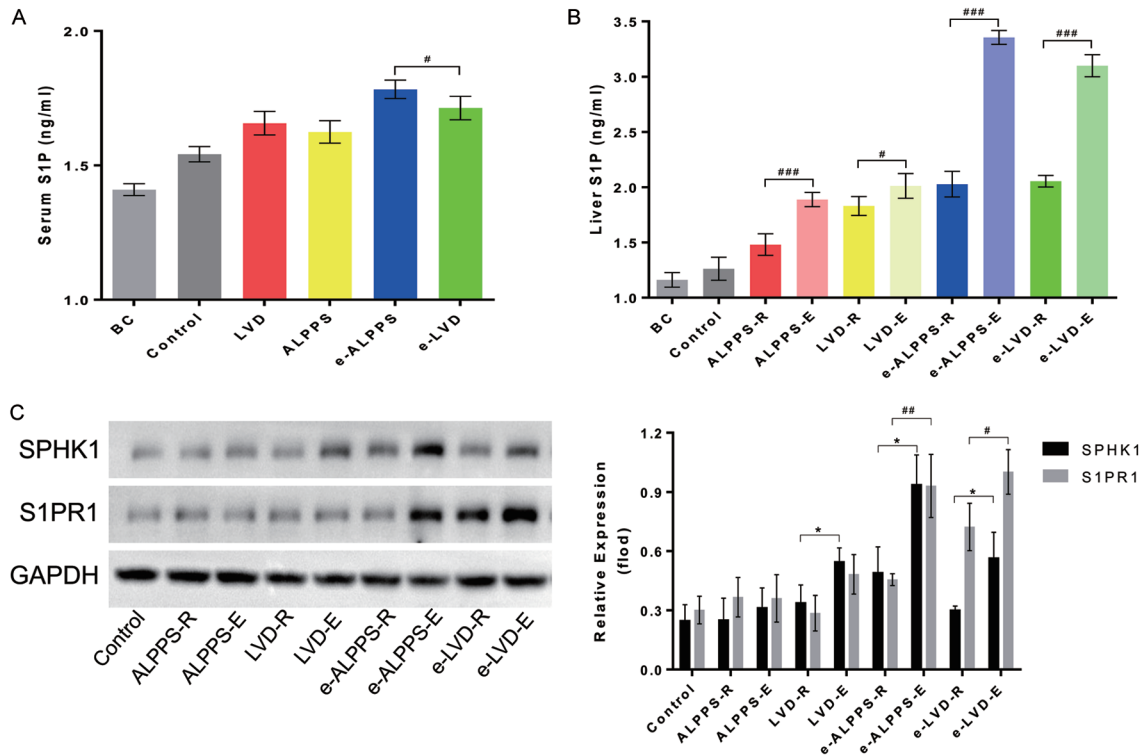


**Fig. 6. Activation of the SPHK1/S1P/S1PR1 pathway.** (A) Serum S1P on POD 2 measured by ELISA. (\*ALPPS vs. LVD; #e-ALPPS vs. e-LVD. \* or # $p < 0.05$ ; \*\* or ## $p < 0.01$ ; \*\*\* or ### $p < 0.001$ ). (B) Liver S1P on POD 2 measured by ELISA. FLR (R) and FLE (E) are shown. (#FLR vs. FLE. # $p < 0.05$ ; ## $p < 0.01$ ; ### $p < 0.001$ ). (C) SPHK1 and S1PR1 levels in the liver were determined by western blotting with and relative expression is shown in the graph (right panel). (#FLR vs. FLE. # $p < 0.05$ ; ## $p < 0.01$ ; ### $p < 0.001$ ). ALPPS, associating liver partition and portal vein ligation for staged hepatectomy; ELISA, enzyme-linked immunosorbent assay; e-LVD, extended liver venous deprivation; FLE, future liver excised; FLR, future liver remnant; LVD, liver venous deprivation; POD, postoperative day; S1P, sphingosine-1-phosphate; S1PR1, sphingosine-1-phosphate receptor 1; SPHK1, sphingosine kinase 1.

blocked with parenchymal ligation (Figs. 2D, F and 3B). In the ALPPS and LVD groups, the LML and RML were designated the FLR and FLE, respectively. In the e-ALPPS and e-LVD groups, the RML and LML were designated the FLR and FLE, respectively (Table 2).

As expected, the congested area was smaller than the ischemic area in the LVD group. In contrast, the congested area covered and surpassed the ischemic area in the e-LVD group (Fig. 3D). Next, the hypertrophic effects on the FLR were compared between the different groups. The LVD, ALPPS, e-LVD and e-ALPPS techniques induced rapid liver regeneration compared with the control group (Fig. 1A, E, F). The hypertrophic effect of LVD was slightly weaker; however, no significant difference was observed between the ALPPS and LVD groups. Additionally, the hypertrophic effect of e-LVD was significantly lower than that of e-ALPPS (Fig. 1E, F). The shrinkage of area H in the e-LVD group might counteract its hypertrophic effect (Fig. 1A).

In this study, the effects of different procedures on liver damage were also assessed. As shown in Figure 5, venous deprivation increased the levels of liver function markers. Correspondingly, the histological analysis revealed large patchy necrosis in the venous-deprived rat livers, especially in the LVD group (Fig. 4B). In contrast, only spotty necrosis is observed in the venous-deprived liver in humans.<sup>5,6</sup> The difference in liver morphology between humans and rats may partially account for this discrepancy. In addition, it may result from different approaches used to block venous drainage. In the clinic, the HVE procedure is performed by placing an Amplatzer vascular plug in the proximal HV to obstruct its outflow, and the short hepatic veins and venous

collateral pathways still drain the venous-deprived liver.<sup>5,6</sup> In a rat LVD model, the HVL was adopted to block blood flow, and some short hepatic veins were ligated during the HVL procedure, resulting in the venous-deprived lobe suffering from more severe blood stasis and ischemia (Fig. 7A). Consequently, the venous-deprived liver showed more frequent and extensive necrosis.

S1P is a well-known mitogenic factor produced by the phosphorylation of sphingosine and catalyzed by SPHK1, which is abundantly expressed in the liver.<sup>19,20</sup> S1P is implicated in many human health and disease processes, and can promote liver regeneration and fibrosis after injury via its receptors, S1PRs.<sup>19,20</sup> To clarify the molecular mechanisms involved in the liver regeneration of LVD and ALPPS, the SPHK1/S1P/S1PR1 signaling pathway was investigated. Compared with control group, both the serum and liver S1P concentrations in experimental groups were significantly increased, and the S1P levels in FLE were significantly higher than that in FLR (Fig. 6A, B). Western blots showed that the expression of SPHK1 and S1PR were significantly upregulated in the FLE (Fig. 6C). This study indicated that congestion or ischemic injury to the FLE activated the SPHK1/S1P/S1PR1 signaling pathway, which promoted the proliferation of hepatocytes in the FLR and mediated fibrosis in the FLE.

The necessity of removing the LLL and the relatively high mortality rate of the e-LVD model should be emphasized. The LLL was preserved when building the e-LVD model in preliminary experiments, which led to substantial congestion of the LLL, LML, and part of the RML, and a large amount of blood accumulated in the liver. Consequently, all the rats died of ischemic shock during the operation. Consequently,

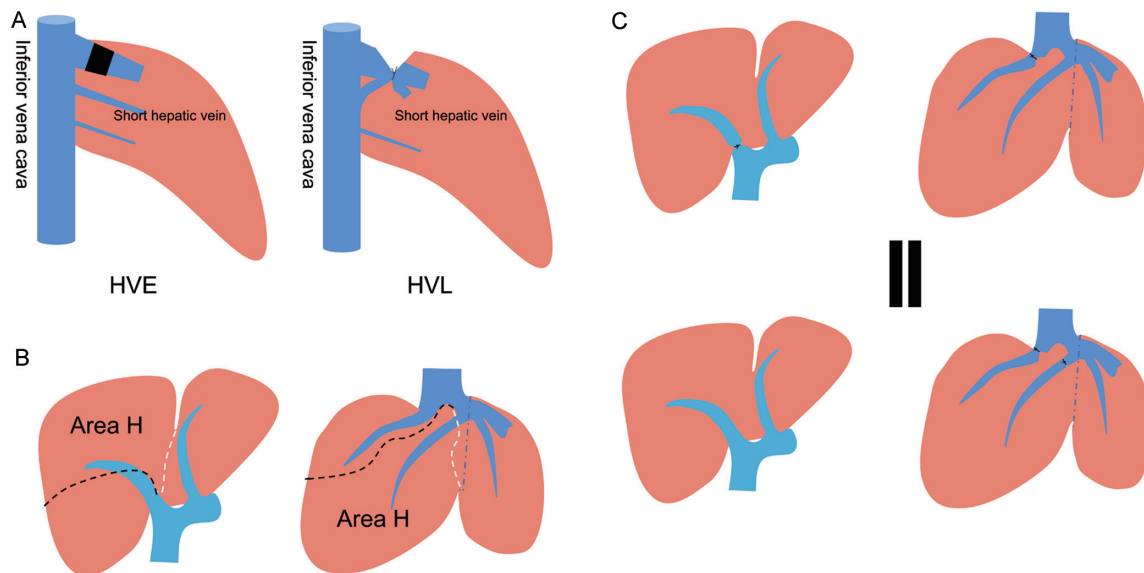


**Fig. 7. Schematic illustrations.** (A) Some short hepatic veins were occluded during the HVL procedure (right panel) but were unaffected during the HVE procedure (left panel). (B) Area H refers to the hybrid area that is supplied by the RMPV and drained by the MMHV, which merges with the LMHV. The dividing line between the supply territories of the RMPV and LMPV (white dotted line) and the dividing line between the drainage areas of the RMHV and MMHV (black dotted line) are shown. Area H is the sector surrounded by the dotted lines. (C) HVL alone or HVL/PVL produced similar results when choosing the proper lobes. HVE, hepatic vein embolization; HVL, hepatic vein ligation; LMHV, left median hepatic vein; LML, left median lobe; LMPV, right median portal vein; MMHV, middle median hepatic vein; PVL, portal vein ligation; RMHV, right median hepatic vein; RMPV, right median portal vein.

the LLL was removed when generating the e-LVD model. All the e-LVD rats received an injection of 6 ml of GS solution, and the survival rate reached approximately 80%. However, the relatively high mortality rate of the e-LVD procedure has not been reported in patients. The discrepancy in mortality may be related to differences in the liver anatomy between rats and humans. In rats that underwent the e-LVD procedure, the congested liver/total liver ratio may be greater than the ratio in patients, and the relatively larger area of liver congestion led to less blood in the circulation. On the other hand, removal of the LLL and CL as well as serious liver congestion triggered severe hepatic dysfunction that manifested as a low ALB level (Fig. 5C), which further aggravated hypovolemia.<sup>21</sup> As a result, the e-LVD rat models had a higher mortality rate than the patients.

The Tp-ALPPS technique was also first applied to a rat model by parenchymal ligation. Many different rat ALPPS models have been described in previous publications, and the parenchyma between the LML and RML was transected in all of those models.<sup>22–24</sup> Combining three-dimensional reconstruction of the liver vascular system with practical experience, Wei *et al.*<sup>23</sup> reported that the end of parenchymal transection should have a minimal distance of 5 mm from the vena cava to avoid injury to the MMHV and RMHV. On the other hand, the Tp-ALPPS technique has been recently reported.<sup>16</sup> The Tp-ALPPS technique takes advantage of partial ALPPS and tourniquet ALPPS and was designed to ligate the liver parenchyma by placing a tourniquet across the liver parenchyma, which achieved a similar increase in volume as tourniquet ALPPS but with a shorter surgical time.<sup>16,25–27</sup> Based on those studies, parenchymal ligation was conducted in rats in this experiment, and the details are described in the methods. The ligation plane gradually became a necrotic zone in the ALPPS and e-ALPPS groups, the FLR exhibited noticeable hypertrophy, and the FLE exhibited obvious atrophy (Fig. 1A). The postoperative changes in the rat models were consistent with those observed in practice.<sup>27</sup> In addition, the parenchymal ligation technique was time-saving and potentially prevented massive hemorrhage

during the parenchymal transection procedure.

Finally, the changes in area H in the e-LVD group should be highlighted (Fig. 7B). Only the HV outflow of area H was occluded, its blood inflow was intact, and area H was confirmed to be necrotic (Fig. 1A). The congested liver has been confirmed to spontaneously recover from focal HV outflow obstruction in both rat models and humans. Hemodynamic changes have been systematically investigated in the isolated lobe and unisolated lobe after partial HV occlusion in a rat model.<sup>28,29</sup> For the unisolated lobe (the RML), parenchymal damage in the hyperperfusion area was completely rehabilitated by the formation of intrahepatic veno-venous collateral pathways and vascularized sinusoidal canals. However, for isolated lobes (the LLL), the congested area did not recover, although intrahepatic arterio-portal regurgitation formed, and liver damage was inevitable and serious.<sup>29</sup> Although area H was an unisolated lobe and area H suffered irreversible injury in this experiment, the underlying explanation might be that area H was too large to regenerate by forming veno-venous collaterals. Thus, HVL alone or HVL plus PVL may produce similar results when choosing the proper lobe, and LVD surgery may be substituted with HVE in the clinic (Fig. 7C). However, more experiments are needed to verify this hypothesis.

Several limitations of this study must be acknowledged. First, a methodological limitation of this study is the resection of LLL and CL. Partial resection of the liver itself stimulates hypertrophy in the remnant liver, and resection of the LLL and CL would interfere with the final results to some extent, although resection of the CL and LLL was also performed in the control group. We are attempting to develop a simple and reliable method to ligate the MMHV in which the e-LVD model may combine RMPV ligation and ligation of both the RMHV and MMHV and the LLL is maintained. Another limitation is that partial hepatectomy in the second stage was not performed. The main reason was that the abdominal adhesions induced by the first surgery usually led to diffuse blood oozing in surgical wounds and injury of the bowels during the second surgery. In the clinic, the first step of LVD or e-LVD is

completed with interventional treatment, which prevents the occurrence of abdominal adhesions.<sup>5,6</sup>

So far, clinical experience with LVD or e-LVD procedure is limited. The complications of those new operations are unpredictable, and their treatment effects in complex clinical cases are unknown. The animal model provides us an chance to gained better understanding of LVD or e-LVD. For instance, the high mortality of e-LVD in rat models reminds to take a cautious approach to perform such operations. Because liver fibrosis has a profound influence on liver hemodynamics and regeneration, it is not clear whether the patients with a background of liver cirrhosis are suitable for the LVD procedure. What is more, the impact of LVD on tumor biological behavior is also unclear. Patients undergoing LVD surgery usually wait 2–4 weeks for second stage surgery. Will the LVD induced-hypoxia promote the metastasis of cancer in the portal vein-deprived lobe? Will the LVD induced-congestion facilitate the cancer cells from portal vein system spread to contralateral lobe? In short, the establishment of animal LVD model is helpful for investigating those clinical questions.

## Conclusions

We describe the generation of the first feasible rat model of LVD and e-LVD with simultaneously associated HVL and PVL. The Tp-ALPPS technique was also applied to a rat model by parenchymal ligation for the first time. Both the LVD and ALPPS techniques induced rapid liver regeneration, and LVD and e-LVD had similar overall effects on the volumetric hypertrophic response and strong impacts on liver function. Excessive and thorough venous deprivation may cause severe complications and attenuate liver hypertrophy. The SPHK1/S1P/S1PR1 pathway was involved in the LVD- or ALPPS-induced liver remodeling. The animal models have improved our understanding of liver size regulation and will help us to perform safer and more effective hepatic regeneration techniques.

## Funding

This project was financially supported by the Fundamental Research Funds for the Central Universities (NO. 2042020kf0124) and the National Natural Science Foundation of China (NO. 82001940).

## Conflict of interest

The authors have no conflict of interests related to this publication.

## Author contributions

Study concept and design (YZ, PM, KY), acquisition of data (PM, LX, WB), analysis and interpretation of data (YX, XH), drafting of the manuscript (WS), critical revisions of the manuscript for important intellectual content (XH, KY), and administrative, technical, or material support, study supervision (KY).

## Ethical statement

This animal procedures were approved by the Ethics Committee of the Animal Experiment Center of Wuhan University.

## Data sharing statement

Data and materials are available upon reasonable request to the corresponding author.

## References

- [1] Fernandez H, Nadalin S, Testa G. Optimizing future remnant liver prior to major hepatectomies: increasing volume while decreasing morbidity and mortality. *Hepatobiliary Surg Nutr* 2020;9(2):215–218. doi:10.21037/hbsn.2019.10.24, PMID:32355683.
- [2] Memeo R, Conticchio M, Deshayes E, Nadalin S, Herrero A, Guiu B, *et al*. Optimization of the future remnant liver: review of the current strategies in Europe. *Hepatobiliary Surg Nutr* 2021;10(3):350–363. doi:10.21037/hbsn-20-394, PMID:34159162.
- [3] Kim D, Cormman-Homonoff J, Madoff DC. Preparing for liver surgery with "Alphabet Soup": PVE, ALPPS, TAE-PVE, LVD and RL. *Hepatobiliary Surg Nutr* 2020;9(2):136–151. doi:10.21037/hbsn.2019.09.10, PMID:32355673.
- [4] Lang H, de Santibañes E, Schlitt HJ, Malagó M, van Gulik T, Machado MA, *et al*. 10th Anniversary of ALPPS-Lessons Learned and quo Vadis. *Ann Surg* 2019;269(1):114–119. doi:10.1097/SLA.0000000000002797, PMID:29727331.
- [5] Guiu B, Chevallier P, Denys A, Delhom E, Pierredon-Foulongne MA, Rouanet P, *et al*. Simultaneous trans-hepatic portal and hepatic vein embolization before major hepatectomy: the liver venous deprivation technique. *Eur Radiol* 2016;26(12):4259–4267. doi:10.1007/s00330-016-4291-9, PMID:27090112.
- [6] Guiu B, Quenet F, Escal L, Bibeau F, Piron L, Rouanet P, *et al*. Extended liver venous deprivation before major hepatectomy induces marked and very rapid increase in future liver remnant function. *Eur Radiol* 2017;27(8):3343–3352. doi:10.1007/s00330-017-4744-9, PMID:28101681.
- [7] Laurent C, Fernandez B, Marichez A, Adam JP, Papadopoulos P, Lapuyade B, *et al*. Radiological Simultaneous Portohepatic Vein Embolization (RASPE) Before Major Hepatectomy: A Better Way to Optimize Liver Hypertrophy Compared to Portal Vein Embolization. *Ann Surg* 2020;272(2):199–205. doi:10.1097/SLA.0000000000003905, PMID:32675481.
- [8] Clavien PA. Hepatic Vein Embolization for Safer Liver Surgery: Insignificant Novelty or a Breakthrough? *Ann Surg* 2020;272(2):206–209. doi:10.1097/SLA.0000000000003973, PMID:32675482.
- [9] Sparrelid E, Hasselgren K, Røssok BI, Larsen PN, Schultz NA, Carling U, *et al*. How should liver hypertrophy be stimulated? A comparison of up-front associating liver partition and portal vein ligation for staged hepatectomy (ALPPS) and portal vein embolization (PVE) with rescue possibility. *Hepatobiliary Surg Nutr* 2021;10(1):1–8. doi:10.21037/hbsn.2019.10.36, PMID:33575285.
- [10] Heil J, Korenblik R, Heid F, Bechstein WO, Bemelmans M, Binkert C, *et al*. Preoperative portal vein or portal and hepatic vein embolization: DRAGON collaborative group analysis. *Br J Surg* 2021;108(7):834–842. doi:10.1093/bjs/znaa149.
- [11] Chebaro A, Buc E, Durin T, Chiche L, Brustia R, Didier A, *et al*. Liver Venous Deprivation or Associating Liver Partition and Portal Vein Ligation for Staged Hepatectomy?: A Retrospective Multicentric Study. *Ann Surg* 2021;274(5):874–880. doi:10.1097/SLA.0000000000005121, PMID:34334642.
- [12] van Lienden KP, van den Esschert JW, Rietkerk M, Heger M, Roelofs JJ, Lameris JS, *et al*. Short-term effects of combined hepatic vein embolization and portal vein embolization for the induction of liver regeneration in a rabbit model. *J Vasc Interv Radiol* 2012;23(7):962–967. doi:10.1016/j.jvir.2012.03.011, PMID:22633622.
- [13] Schadde E, Guiu B, Deal R, Kalil J, Arslan B, Tasse J, *et al*. Simultaneous hepatic and portal vein ligation induces rapid liver hypertrophy: A study in pigs. *Surgery* 2019;165(3):525–533. doi:10.1016/j.surg.2018.09.001, PMID:30482517.
- [14] Kawaguchi D, Hiroshima Y, Kumamoto T, Mori R, Matsuyama R, Ichikawa Y, *et al*. Effect of Portal Vein Ligation Plus Venous Congestion on Liver Regeneration in Rats. *Ann Hepatol* 2019;18(1):89–100. doi:10.5604/01.3001.0012.7866, PMID:31113614.
- [15] Sutti S, Tacke F. Liver inflammation and regeneration in drug-induced liver injury: sex matters! *Clin Sci (Lond)*. 2018;132(5):609–613. doi:10.1042/CS20171313, PMID:29545336.
- [16] Robles-Campos R, Brusadín R, López-López V, López-Conesa A, Navarro-Barrios Á, Gómez-Valles P, *et al*. A New Surgical Technique Variant of Partial ALPPS (Tourniquet Partial-ALPPS). *Ann Surg* 2021;273(1):e22–e24. doi:10.1097/SLA.0000000000004244, PMID:32740247.
- [17] Kisseleva T, Brenner D. Molecular and cellular mechanisms of liver fibrosis and its regression. *Nat Rev Gastroenterol Hepatol* 2021;18(3):151–166. doi:10.1038/s41575-020-00372-7, PMID:33128017.
- [18] Chang Y, Li H. Hepatic Antifibrotic Pharmacotherapy: Are We Approaching Success? *J Clin Transl Hepatol* 2020;8(2):222–229. doi:10.14218/JCTH.2020.00026, PMID:32832403.
- [19] Kawai H, Osawa Y, Matsuda M, Tsunoda T, Yanagida K, Hishikawa D, *et al*. Sphingosine-1-phosphate promotes tumor development and liver fibrosis in mouse model of congestive hepatopathy. *Hepatology* 2022;76(1):112–125. doi:10.1002/hep.32256, PMID:34855990.
- [20] Li L, Wang H, Zhang J, Sha Y, Wu F, Wen S, *et al*. SPHK1 deficiency protects mice from acetaminophen-induced ER stress and mitochondrial permeability transition. *Cell Death Differ* 2020;27(6):1924–1937. doi:10.1038/s41418-

- 019-0471-x, PMID:31827236.
- [21] Schumann R, Bonney I, McDevitt LM, Cooper JT, Cepeda MS. Extent of right hepatectomy determines postoperative donor albumin and bilirubin changes: new insights. *Liver Int* 2008;28(1):95–98. doi:10.1111/j.1478-3231.2007.01594.x, PMID:17927715.
- [22] Schlegel A, Lesurtel M, Melloul E, Limani P, Tschuor C, Graf R, *et al*. ALPPS: from human to mice highlighting accelerated and novel mechanisms of liver regeneration. *Ann Surg* 2014;260(5):839–846; discussion 846–7. doi:10.1097/SLA.0000000000000949, PMID:25379855.
- [23] Wei W, Zhang T, Zafarnia S, Schenk A, Xie C, Kan C, *et al*. Establishment of a rat model: Associating liver partition with portal vein ligation for staged hepatectomy. *Surgery* 2016;159(5):1299–1307. doi:10.1016/j.surg.2015.12.005, PMID:26879073.
- [24] Dili A, Lebrun V, Bertrand C, Leclercq IA. Associating liver partition and portal vein ligation for staged hepatectomy: establishment of an animal model with insufficient liver remnant. *Lab Invest* 2019;99(5):698–707. doi:10.1038/s41374-018-0155-z, PMID:30666050.
- [25] Peng SY, Wang XA, Huang CY, Zhang YY, Li JT, Hong DF, *et al*. Evolution of associating liver partition and portal vein ligation for staged hepatectomy: Simpler, safer and equally effective methods. *World J Gastroenterol* 2017;23(23):4140–4145. doi:10.3748/wjg.v23.i23.4140, PMID:28694654.
- [26] Robles Campos R, Parrilla Paricio P, López Conesa A, Brusadín R, López López V, Jimeno Griñó P, *et al*. [A new surgical technique for extended right hepatectomy: tourniquet in the umbilical fissure and right portal vein occlusion (ALTPS). Clinical case]. *Cir Esp* 2013;91(10):633–637. doi:10.1016/j.ciresp.2013.09.004, PMID:24246509.
- [27] Robles R, Parrilla P, López-Conesa A, Brusadín R, de la Peña J, Fuster M, *et al*. Tourniquet modification of the associating liver partition and portal ligation for staged hepatectomy procedure. *Br J Surg* 2014;101(9):1129–1134; discussion 1134. doi:10.1002/bjs.9547, PMID:24947768.
- [28] Huang H, Deng M, Jin H, Liu A, Dirsch O, Dahmen U. Hepatic arterial perfusion is essential for the spontaneous recovery from focal hepatic venous outflow obstruction in rats. *Am J Transplant* 2011;11(11):2342–2352. doi:10.1111/j.1600-6143.2011.03682.x, PMID:21831159.
- [29] Tan X. Hemodynamic remodeling mechanism and pathophysiological correlate in rat hepatic vein outflow obstruction [Chinese]. Chinese PLA General Hospital & Medical School 2013.